APL Materials

High performing designer glass platform to host versatile photonic devices

Cite as: APL Mater. 9, 121109 (2021); https://doi.org/10.1063/5.0063788
Submitted: 17 July 2021 • Accepted: 09 November 2021 • Published Online: 20 December 2021

T. Toney Fernandez, Simon Gross, Alexander Arriola, et al.

High performing designer glass platform to host versatile photonic devices

Cite as: APL Mater. 9, 121109 (2021); doi: 10.1063/5.0063788
Submitted: 17 July 2021 • Accepted: 9 November 2021 •
Published Online: 20 December 2021

T. Toney Fernandez,[1,a)] Simon Gross,[1] Alexander Arriola,[1] Karen Privat,[2] and Michael J. Withford[1]

AFFILIATIONS

[1] MQ Photonics Research Centre, Department of Physics and Astronomy, Macquarie University, Sydney, NSW 2109, Australia

[2] Electron Microscope Unit, Mark Wainwright Analytical Centre, University of New South Wales, Sydney, Australia

[a)] **Author to whom correspondence should be addressed:** toney.teddyfernandez@mq.edu.au

ABSTRACT

The aluminum to alkaline earth ratio (Al:[AE]) in borosilicate glass is introduced as a novel compositional parameter to produce high index waveguides through femtosecond laser inscription. Alkaline earths are considered to be major refractive index providers for laser written optical waveguides due to their collective migration toward the guiding region. Contrary to the existing belief that increasing the concentration of such index providers within a glass composition will help to produce high index change waveguides, we demonstrate that high index waveguides can be fabricated by tuning the Al:[AE] ratio while keeping the absolute concentration of the index provider to a minimum.

I. INTRODUCTION

Integral to our modern optical communication networks are integrated photonic circuits that switch, split, route, and modulate data streams that are crisscrossing our planet carried in optical fibers. Driven by the need for ever higher data rates in the telecommunication sector, we have witnessed tremendous innovation in the field of integrated photonics.[1,2] The quest for miniaturization, integration, scalability, and efficiency has seen the adoption of lithographic fabrication processes that were initially developed for integrated electronic circuits to create photonic circuits, most notably CMOS compatible silicon photonics.[3] The innovation in the past few decades has paved the way for potentially novel mass applications for integrated photonics beyond optical communication, such as life science[4] or LIDAR for autonomous vehicles.[5] Ultrafast laser inscription enables the creation of integrated photonic circuits with true rapid three-dimensional prototyping functionality.[6] Glass is the major dielectric platform to host such intricate devices. The parameter space to produce waveguides in glass is governed by the way laser energy is deposited in the material, i.e., the laser repetition rate, pulse energy, inscription feed rate, and focusing conditions. Thus, optimizing the inscription parameters is a standard procedure, but the influence of the glass composition on the said parameter space should not be overlooked. Recently, it was demonstrated that modifying the glass composition could be a way around the bottle necking of the index change and morphological tuning of waveguides to reduce loss and attain high performing devices.[7] However, a full understanding of waveguide formation behavior is missing, and hence, pinpointing a compositional parameter has not been possible. In a recent report using commercial glasses, we have identified that optimizing the Al:[AE] = $\frac{Al_2O_3}{Al_2O_3+CaO}$ ratio is a key to produce waveguides with a high index change and circular morphology.[8] Here, we take a step forward to test this hypothesis; for this study, we fabricated four custom alkaline earth boro-aluminosilicate glasses with different Al:[AE] ratios and used these to confirm that a new compositional parameter exists that can be used to tune waveguide properties. In commercial alkaline earth boro-aluminosilicate glasses, Ca and Al were identified as the refractive index providers for fs-laser written waveguides.[9] An intuitive approach would be to increase the Ca and Al content to yield a higher index change in fabricated waveguides. However, this report confirms that such a practice would not bring the intended results. We demonstrate that waveguides with a positive refractive index change higher than 1×10^{-2} inscribed at a feed rate as high as 2000 mm/min can be fabricated simply by tuning the Al:[AE] ratio to greater than

0.5 (peraluminous composition) while keeping the absolute content of CaO to a minimum.

II. METHODS

Boro-aluminosilicate glasses were fabricated using the melt quenching technique. Four glasses with different compositions as tabulated in Table I were melted at a temperature of 1650 °C. After melting, glasses were annealed at a temperature of 750 °C and then cut and polished to obtain a high optical surface quality for laser inscription. The samples are coded according to the aluminum to alkaline earth (Al:[AE]) ratio. All waveguides in this study were written using a 5.1 MHz high-repetition rate Ti:sapphire chirped-pulse femtosecond oscillator (Femtosource XL500, Femtolasers GmbH), emitting 50 fs pulses and operating at a wavelength of 800 nm. Circularly polarized laser pulses were focused inside the glass using an Olympus UPLANSAPO 100× oil immersion microscope objective (NA = 1.4), which is aberration corrected at a depth of 170 μm. Waveguides were written at that particular depth using a set of three-axis computer-controlled high precision Aerotech air-bearing linear stages. Since the waveguides are purely written in a heat accumulation regime, an isotropic heat diffusion is expected from this aberration corrected laser focal spot to produce circular structures. All glasses were investigated under identical experimental conditions. As a control measure to aid comparison, identical 30 μm diameter structures were inscribed in all glasses by adjusting the pulse energy for each feed rate of 100, 200, 500, 1000, and 2000 mm/min (1.67, 3.33, 8.33, 16.67, and 33.33 mm/s, respectively). This means that in each glass and for each feed rate, the deposited energy was adjusted to result in a temperature distribution where at a distance of 15 μm away from the focal spot, the temperature was insufficient to induce any further refractive index modification. We define the quenching time as the time it takes for the glass to cool from the peak temperature at the focal spot to a temperature that does not result in any further refractive index modification. This corresponds to the time it takes for the sample to move by 15 μm at a given feed rate. The resulting quenching times are 9, 4.5, 1.8, 0.9, and 0.45 ms at a feed rate of 100, 200, 500, 1000, and 2000 mm/min, respectively.

Despite being small batch samples, the intrinsic internal loss of the glass was as low as 0.09 dB/cm for Al:[AE]0.52 after subtracting the Fresnel losses (Fig. 1). The loss values are bit higher compared to the ones reported in commercial boro-aluminosilicate Corning Eagle 2000/XG and Schott AF45 glasses.[10] We believe that the losses are due to the striae and associated density inhomogeneities after quenching the glass. The loss values were found to reduce with

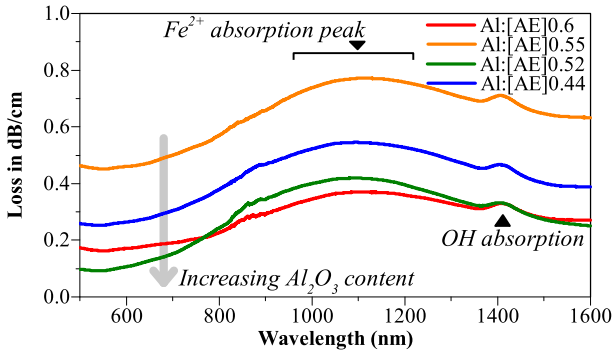

FIG. 1. Internal losses in dB/cm for the glass samples after correction for the Fresnel losses.

increasing aluminum content. This is because aluminum inhibits phase separations between the glass formers, SiO_2 and B_2O_3, promoting the intermixing of both and producing B–O–Al–O–Si linkages.[11] This results in a highly miscible melt before it is quenched. The losses could be improved by increasing the batch volume to facilitate a more homogeneous thermal profile during quenching. The broad peak found centered around 1100 nm is due to the presence of Fe^{2+} ions within the glass.[10,12] Inclusion of the undesirable iron within the glass is usually from the raw materials and could be completely removed by using high purity (99.999%/5 N) precursors. Regarding the general properties of the glass compositions produced here since SiO_2 and B_2O_3 are the glass formers and the variation of their ratio is kept minimal across different compositions, their effects on the coordination number on the glass and the formation of nonbridging oxygen units are negligible. Al_2O_3 and CaO absolute mol. % values are varied moderately; this can directly affect the viscosity and production of nonbridging oxygen (NBO) and change the boron coordination. Addition of Al_2O_3 in such a composition assumes a higher responsibility in imparting an ionic character to the B–O network, facilitating the formation of B–O–Al–O–Si and thereby increasing the compatibility of the Si network with the B–O network. The effect of viscosity when both Al_2O_3 and CaO are present then depends on the influence of the coordination number of boron. A higher coordination number is expected when modifiers with higher valences are available for charge balance, which stabilize the boron network. However, since the bond energy of four-coordinated boron is stronger than a three-coordinated one [when the influence of low valence modifiers (alkali, alkaline earths) has an

TABLE I. Glass compositions in mol. % and their corresponding density and refractive indices used in this work.

Sample name	Al:[AE]0.55	Al:[AE]0.6	Al:[AE]0.44	Al:[AE]0.52
$Al:[AE] ratio$	0.55	0.6	0.44	0.52
SiO_2	68.7	66.7	61.2	59.7
B_2O_3	8.3	8.4	9.5	5.6
Al_2O_3	12.2	14.4	12.6	17.4
CaO	9.8	9.5	15.8	16.2
Density(g/cc)	2.36	2.41	2.43	2.44
Index (n_D)	1.508	1.515	1.52	1.529

upper hand], the former is easier to break, reducing the viscosity of the melt at a particular temperature.

Images of the end-faces were recorded using an Olympus IX81 inverted optical microscope in the differential interference contrast mode. The refractive index profiles of the waveguides were recorded using the refracted-near-field technique (RINCK Elektronik) at a wavelength of 635 nm. SEM imaging and electron probe microanalysis (EPMA) mapping of ion migration were carried out on a JEOL JXA-8500F field-emission EPMA at an accelerating voltage of 15 kV and a probe current of 20 nA in the beam scan mode.

III. RESULTS AND DISCUSSION

The differential interference contrast microscopic images of the 30 μm diameter waveguides formed in two different glasses with Al:[AE] = 0.6 and 0.44 are shown in Fig. 2. Waveguides written with feed rates of 100, 200, 500, and 2000 mm/min are provided to demonstrate the evolution of the morphology due to different quench rates. A typical waveguide structure can be identified as the central heat accumulated region (core) and the heat diffused region (halo) surrounding the core. Sample Al:[AE]0.6 stands out in terms of its contrast and highly circular morphology that was maintained for all feed rates ranging between 200 and 2000 mm/min. Waveguides in Al:[AE]0.44 and other glasses demonstrated a non-circular vertically elongated inverted tear drop shape. The morphological variation could not be due to spherical aberrations during waveguide inscription resulting from different refractive indices between the glasses as (1) all the waveguides were written at the same 170 μm depth and (2) the index of Al:[AE]0.6 glass (1.515) was higher than that of Al:[AE]0.55 (1.508) and lower than that of Al:[AE]0.44 (1.52) and Al:[AE]0.52 glasses (1.529) (Table I). The positive refractive index change [$n_{max\ (positive)} - n_{bulk}$] and the refractive index contrast [$n_{max\ (positive)} - n_{min\ (negative)}$] values obtained for waveguides written between 100 and 2000 mm/min feed rate for all glasses are shown in Figs. 3(a) and 3(b).

Glass with the highest Al:[AE] ratio outperformed the other three, producing a positive index change of 1.06×10^{-2} and a contrast of 1.38×10^{-2} for a feed rate of 500 mm/min. In fact, the positive index change obtained for all the four glasses for the feed rates between 200 and 2000 mm/min is of the same ascending order as the Al:[AE] ratio, Al:[AE]0.6 > Al:[AE]0.55 > Al:[AE]0.52 > Al:[AE]0.44. The origin of this index change for these feed

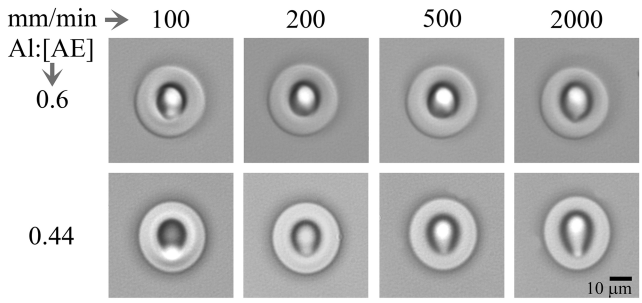

FIG. 2. DIC images of Al:[AE] = 0.6 and 0.44 glass waveguides (30 μm) written with feed rates of 100, 200, 500, and 2000 mm/min. The inscription laser was incident from the top.

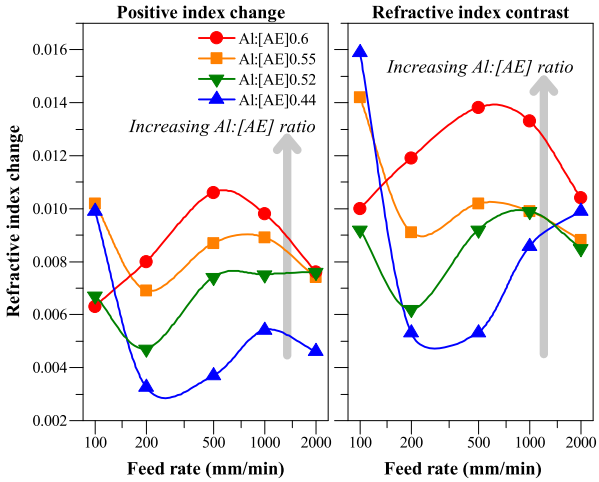

FIG. 3. Positive index change and the refractive index contrast obtained for the 30 μm waveguides written in all four borosilicate glasses.

rates was investigated with electron probe microanalysis (EPMA). It was observed that the densified core was enriched in calcium and aluminum and the first concentric ring, which is the negative index change zone, was enriched in silicon (Fig. 4). Even though aluminum and calcium were the classic refractive index providers (through core densification) in these glasses, the magnitude of the positive refractive index change obtained did not follow the molar content of Ca or Al within the glass composition. CaO and Al_2O_3 concentrations were 16.2 and 17.4 mol. % in Al:[AE]0.52 and 15.8 and 12.6 mol. % in Al:[AE]0.44, respectively. Both these glasses performed poorly in achieving a strong refractive index change within the laser written waveguides when compared to the other glasses. The relative atomic weight difference between Ca (40.078) and Al (26.982) is almost 39%. Hence, Ca is the major driver of densification and higher index change within the waveguide core. However, surprisingly, the highest positive index change waveguides were formed in Al:[AE]0.6 glass, which exhibits the lowest Ca content of all the samples (9.5 mol. %). Figure 5 provides a complete two-dimensional profile of the waveguide (500 mm/min) with the maximum index change (1.06×10^{-2}) obtained in the Al:[AE]0.6 sample.

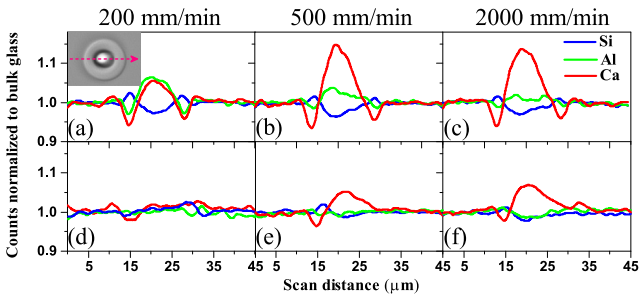

FIG. 4. Migration of Si, Ca, and Al in (a)–(c) Al:[AE]0.6 and (d–f) Al:[AE]0.44 for feed rates of 200, 500, and 2000 mm/min. Inset: DIC image of the waveguide written with the 200 mm/min feed rate in Al:[AE]0.6 glass and the red arrow indicates the EPMA scan direction that also corresponds to the fs-laser inscription direction.

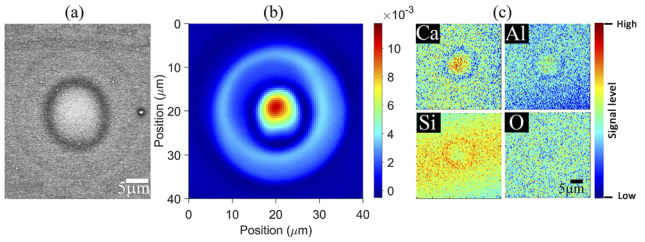

FIG. 5. (a) BSE image, (b) refractive index profile, and (c) elemental maps of waveguides written in Al:[AE]0.6 at a feed rate of 500 mm/min.

Figure 5(a) shows the backscattered electron (BSE) image; the relatively bright pixels within them indicate densification, which is due to the segregation of heavier atomic weight elements (Z-contrast). The dark pixels indicate rarefaction compared to the surrounding unmodified region and are mostly due to the outward migration of relatively heavy elements. The core region of all waveguides indicates that it is formed due to material densification, and the first concentric ring is due to low material density. The halo is also featured in the BSE image as weak densification. This is caused by a frozen-in stress pattern where glass constituents are stacked closer together compared to the prestine bulk in contrast to ion-migration related densification.[9] Figure 5(b) shows the refractive index profile, and Fig. 5(c) identifies the densification of the core due to the accumulation of Ca and Al, while the first concentric ring is formed due to the migration of silicon to this area. No significant trends in oxygen distribution were identified. The trend of migration was the same in all waveguides in all glasses except only for the variation in the signal intensity.

The results show that the aluminum to alkaline earth ratio is the primary factor responsible for a densification/high index change in boro-aluminosilicate glass modified by alkaline earths. To date, the understanding of the migration of elements within a dielectric upon femtosecond laser exposure has been limited. Information from previous studies could be summarized as (1) glass forming elements (silicon) migrate to the focal point (highest temperature),[13] (2) SiO_2 migrates to the hot (cold) side in SiO_2-rich (poor) composition due to an existing negative (positive) Soret coefficient with a reversal of this trend occurring around 20 mol. %,[14,15] and (3) elements with monovalancy tend to migrate toward higher defect density within a glass.[16] The first two conclusions are based on static irradiation of glass by femtosecond laser, with the observation of elemental migration made perpendicular to the laser beam direction. The third point is based on dynamic irradiation where a waveguide is being inscribed by translating the glass perpendicular to the laser beam, with the observation made at the transverse section of waveguides. It has also been demonstrated that the migration direction depends on the thermal profile of the laser plasma.[17] However, it has not been shown until now that the elemental migration within a glass composition modified with alkaline earth can be sensitized/activated simply by changing the aluminum to alkaline earth ratio of the base glass composition. This contradicts the conventional view that adding more refractive index providers to the glass composition (Ca for E2K, EXG, AF32, and 1737F; Sr for OA-10G and 1737F; and Ba for AF32, AF45, 7059F, and 1737F)[8] will increase the refractive index contrast for waveguides. When the Al:[AE] ratio is >0.5, the glass is in a peraluminous composition where aluminum balances every mole of alkaline earth within the glass. In contrast, when Al:[AE] = <0.5, it is a peralkaline composition where aluminum is outnumbered. Peralkaline glasses are always characterized by sharp viscosity changes with temperature,[18] wherein a peraluminous composition of the viscosity variation is very subtle over a wide range. We have earlier reported the importance of having a high melt viscosity that induces strong alkaline earth ion migration in Corning Eagle and Schott Alkali-Free (AF) glasses to provide high index change waveguides.[9] Calcium, which is the main alkaline earth metal used in our composition, has a higher diffusivity by several orders of magnitude at high viscosities.[19] The composition-dependence of Ca diffusivity has a slight positive dependence on the SiO_2 content. Therefore, it is expected that Ca has a higher diffusivity in Al:[AE]0.6 (66.7 mol. % SiO_2) composition than in Al:[AE]0.44 (61.2 mol. % SiO_2).

A detailed interpretation to pin point the immediate cause of elemental migration behavior at this stage is difficult as tracking the behavior of Ca and Al associated with this phenomenon on a micrometer-sized scale like an optical waveguide involves analyzing rapid atomic scale interactions and therefore meets with severe characterization constraints. Highly resolving techniques that could pin point the coordination statistics of oxygen due to the presence of Si, Al, and Ca such as nuclear magnetic resonance or x-ray scattering techniques have a sampling volume of tens of microns. Although Raman spectroscopy is sensitive to the changes due to network modifiers, broad vibrational responses that arise from a highly amorphous bulk matrix are often difficult to differentiate, analyze, and interpret. Nevertheless, based on previous studies of calcium aluminosilicate glasses, we believe that in a peraluminous composition in addition to the higher diffusivity attained by the calcium, there is a favorable environment to form more Ca–O–Si bonds compared to that of a peralkaline composition. It is known that in a peralkaline composition, silicon-nonbridging oxygen (NBO) formation is energetically more favorable than Al-NBO formation; it therefore follows that in a peraluminous composition, Al-NBO formation could be possible. The presence of Ca^{2+} stabilizes the formation of Al–O–Al, which would otherwise be energetically less favorable compared to the formation of Al–O–Si.[20] Hence, in peraluminous composition, the probability of forming Ca–O–Al is higher but would be accompanied by an energy penalty of 108 kJ/mol compared to the formation of Ca–O–Si.[21] Due to the external energy deposition from the laser, especially at the core where it is the maximum, such a penalty could be easily overcome and a favorable environment is created for the migration of calcium toward the core. Within the core, quenching occurs on much faster time scale, further facilitating the freeze-in of non-equilibrium structures. This is demonstrated in the migration of calcium strongly paired with aluminum (green curves in Fig. 4) in peraluminous glasses compared to the peralkaline glass.

IV. CONCLUSION

Production of ultrafast laser written waveguides that are governed by the elemental migration of glass constituents is carried out in this study. The aluminum to alkaline earth ratio is used as a compositional parameter in a borosilicate glass to produce high refractive index waveguides. Specific glass forming or modifying elements are considered to be refractive index providers for optical

waveguides due to their collective migration toward the guiding region to form a densified zone. The existing reports suggest that tuning the glass composition to increase such index providing elements can produce waveguides with high index changes. In this report, we have shown that such compositional tuning can lead to the results that are contrary to the expectations. Calcium and aluminum are known to be the refractive index providers for waveguide formation in an alkaline earth boro-aluminosilicate glass, wherein Ca plays a dominant role due to its relatively high atomic weight. Experiments carried out in four different glasses with different aluminum to calcium (Al:[AE]) ratios demonstrated that high Al:[AE] rather than high Ca content produced waveguides with a high index change ($>1 \times 10^{-2}$). Glass with a high Al:[AE] ratio was purposefully chosen to have the least Ca content to test this concept. Our results suggest that the primary drivers facilitating this phenomenon are twofold: (1) high viscosity with the minimal localized gradient during waveguide formation in glass samples with the Al:[AE] ratio >0.5 and (2) increased diffusivity of calcium and favorability of Ca–O–Al unit formation within the core due to peraluminous composition. Hence, to conclude, high performing waveguides could be designed in a pre-designed glass that exploits all these learnings, whose properties could be easily tuned by changing one or a combination of the inscription parameters, such as laser energy, feed rate, repetition rate, and/or the focusing condition, thanks to the extensive parameter space offered by femtosecond laser inscription along with exceptional control with a novel pre-emptive glass design.

ACKNOWLEDGMENTS

This work was performed, in part, at the OptoFab node of the Australian National Fabrication Facility, utilizing NCRIS and NSW state government funding. This project was supported by the Australian Research Council under its Discovery Project Program (Grant Nos. DP170104644, DE160100714, and FT200100590). The authors acknowledge the use of facilities supported by Microscopy Australia at the Electron Microscope Unit within the Mark Wainwright Analytical Centre at UNSW Sydney.

AUTHOR DECLARATIONS

Conflict of Interest

The authors have no conflicts to disclose.

DATA AVAILABILITY

The data that support the findings of this study are available from the corresponding author upon reasonable request.

REFERENCES

[1] J. M. Kahn and D. A. B. Miller, "Communications expands its space," Nat. Photonics **11**, 5–8 (2017).
[2] D. A. B. Miller, "Attojoule optoelectronics for low-energy information processing and communications," J. Lightwave Technol. **35**, 346–396 (2017).
[3] D. J. Blumenthal, "Photonic integration for UV to IR applications," APL Photonics **5**, 020903 (2020).
[4] J. Witzens, P. Leisching, A. T. Mashayekh, T. Klos, S. Koch, F. Merget, D. Geuzebroek, E. Klein, T. Veenstra, and R. Dekker, "Photonic integrated circuits for life sciences," arXiv:2101.05368 [physics.ins-det] (2020).
[5] M. J. Heck, "Highly integrated optical phased arrays: Photonic integrated circuits for optical beam shaping and beam steering," Nanophotonics **6**, 93–107 (2017).
[6] R. Osellame, G. Cerullo, and R. Ramponi, *Femtosecond Laser Micromachining: Photonic and Microfluidic Devices in Transparent Materials* (Springer, 2012).
[7] T. T. Fernandez, M. Sakakura, S. M. Eaton, B. Sotillo, J. Siegel, J. Solis, Y. Shimotsuma, and K. Miura, "Bespoke photonic devices using ultrafast laser driven ion migration in glasses," Prog. Mater. Sci. **94**, 68–113 (2018).
[8] T. T. Fernandez, S. Gross, K. Privat, B. Johnston, and M. Withford, "Designer glasses—Future of photonic device platforms," Adv. Funct. Mater. (published online 2021).
[9] T. T. Fernandez, S. Gross, A. Arriola, K. Privat, and M. J. Withford, "Revisiting ultrafast laser inscribed waveguide formation in commercial alkali-free borosilicate glasses," Opt. Express **28**, 10153–10164 (2020).
[10] T. Meany, S. Gross, N. Jovanovic, A. Arriola, M. J. Steel, and M. J. Withford, "Towards low-loss lightwave circuits for non-classical optics at 800 and 1,550 nm," Appl. Phys. A **114**, 113–118 (2014).
[11] W.-F. Du, K. Kuraoka, T. Akai, and T. Yazawa, "Study of Al_2O_3 effect on structural change and phase separation in Na_2O-B_2O_3-SiO_2 glass by NMR," J. Mater. Sci. **35**, 4865–4871 (2000).
[12] L. B. Glebov and E. N. Boulos, "Absorption of iron and water in the Na_2O–CaO–MgO–SiO_2 glasses. II. selection of intrinsic, ferric, and ferrous spectra in the visible and UV regions," J. Non-Cryst. Solids **242**, 49–62 (1998).
[13] S. Kanehira, K. Miura, and K. Hirao, "Ion exchange in glass using femtosecond laser irradiation," Appl. Phys. Lett. **93**, 023112 (2008).
[14] M. Shimizu, J. Matsuoka, H. Kato, T. Kato, M. Nishi, H. Visbal, K. Nagashima, M. Sakakura, Y. Shimotsuma, H. Itasaka, K. Hirao, and K. Miura, "Role of partial molar enthalpy of oxides on Soret effect in high-temperature CaO–SiO_2 melts," Sci. Rep. **8**, 15489 (2018).
[15] M. Shimizu, T. Fukuyo, J. Matsuoka, K. Nakashima, K. Sato, T. Kiyosawa, M. Nishi, Y. Shimotsuma, and K. Miura, "Determination of thermodynamic and microscopic origins of the Soret effect in sodium silicate melts: Prediction of sign change of the Soret coefficient," J. Chem. Phys. **154**, 074501 (2021).
[16] T. T. Fernandez, B. Sotillo, J. del Hoyo, J.-A. Vallés, R. M. Vázquez, P. Fernandez, and J. Solis, "Dual regimes of ion migration in high repetition rate femtosecond laser inscribed waveguides," IEEE Photonics Technol. Lett. **27**, 1068–1071 (2015).
[17] T. T. Fernandez, J. Siegel, J. Hoyo, B. Sotillo, P. Fernandez, and J. Solis, "Controlling plasma distributions as driving forces for ion migration during fs laser writing," J. Phys. D: Appl. Phys. **48**, 155101 (2015).
[18] B. O. Mysen, D. Virgo, and F. A. Seifert, "The structure of silicate melts: Implications for chemical and physical properties of natural magma," Rev. Geophys. **20**, 353–383, https://doi.org/10.1029/rg020i003p00353 (1982).
[19] D. B. Dingwell and S. L. Webb, "Relaxation in silicate melts," Eur. J. Mineral. **2**, 427–449 (1990).
[20] S. K. Lee and J. F. Stebbins, "The degree of aluminum avoidance in aluminosilicate glasses," Am. Mineral. **84**, 937–945 (1999).
[21] S. K. Lee and J. F. Stebbins, "Disorder and the extent of polymerization in calcium silicate and aluminosilicate glasses: O-17 NMR results and quantum chemical molecular orbital calculations," Geochim. Cosmochim. Acta **70**, 4275–4286 (2006).